Arabian Journal of Geosciences (2020) 13: 1192
https://doi.org/10.1007/s12517-020-06174-0

ORIGINAL PAPER

Palynofacies analysis and source rock evaluation of the Upper Cretaceous-Oligocene succession in the Drazia-1 well, Alamein Basin, Egypt

Omar Mohamed[1] · Fathyia Mahdy[1] · Sameh S. Tahoun[2]

Received: 26 August 2020 / Accepted: 26 October 2020 / Published online: 9 November 2020

Abstract

Visual palynofacies analysis and petroleum source rock assessment are reliable and widely used applications for hydrocarbon potential. The Alamein Basin located in the north Western Desert is one of the promising hydrocarbon provinces all over Egypt. In this context, a total of 59 cutting samples representing the Upper Cretaceous Khoman formation and the Paleocene-Oligocene Apollonia and Dabaa rock units from the Drazia-1 well drilled in the East Yidma Oil Field, Alamein Basin, were analyzed. These samples were investigated for their palynological and palynofacies microscopy, including 39 samples for geochemical screening of their organic carbon content and 10 samples for Rock-Eval® 6 Turbo. Palynofacies analysis defined two palynofacies types of organic matter (OM). The first was characterized by phytoclasts-AOM composition of kerogen type III (gas-prone) and represents the Dabaa and Apollonia formations, and was deposited in a highly proximal shelf setting in marginal oxic-dysoxic conditions. The second was dominated by amorphous organic matter (AOM) and recognized in the Khoman formation, demonstrating a distal suboxic-anoxic basin with oil-prone kerogen type II. Moreover, geochemical analyses of the total organic carbon (TOC) content and the Rock-Eval pyrolysis determine the characteristics of possible source rock intervals and defined their hydrocarbon potentials. The investigated interval (4200–5150 ft) is suggested to be a poor source rock due to poor hydrocarbon potential of S_2 values. The organic matter was thermally immature of kerogen type III (woody material typically generates gas). The palynofacies distributions and thermal hydrocarbon maturation in the Alamien Basin were affected by the tectonic movements that happened in the northern Egypt, mainly the Syrian Arc System.

Keywords Kerogen type · Thermal maturity · Hydrocarbon generating potential · Alamien Basin · Western Desert · Egypt

Introduction

The subsurface Cretaceous sediments cover a wide area of the Northern Western Desert of Egypt and include many structurally controlled sedimentary basins where various rock facies were deposited. Western Desert has exceptional hydrocarbon potentiality and is considered an important oil province in Egypt. The north Western Desert tectonically lies in the unstable shelf (Hantar 1990). This area is characterized by two main fault trends: the first formed contemporaneous with the opening of the Neo-Tethys corresponds the Jurassic rift, and the second corresponds the Cretaceous faults. This is accompanied by periods of compressive tectonism (Deformation of the Syrian Arc). Another important aspect was the dextral or sinistral rotation of the North African plate relative to Laurasia, which had a robust modifying effect on the regional tectonic basin styles encountered in North East Africa, especially the Western Desert (EGPC 1992). Western Desert comprises eight Mesozoic basins (Shushan, Matruh, Kattaniya, Qattara, Dahab-Mireir, Natrun, Alamein, and Abu Gharadig) and a Tertiary basin (Gindi Basin). The Western Desert has been subjected for several palynological, organic geochemical, and hydrocarbon potential studies. Palynological studies play a great role currently in upstream sector. In Egypt, these investigations were started by the work of Urban et al. (1976) and followed by a series of authors (e.g.,

Responsible Editor: Santanu Banerjee

✉ Omar Mohamed
omar.mohamed@mu.edu.eg

[1] Faculty of Sciences, Geology Department, Minia University, El-Minia, Egypt

[2] Faculty of Science, Geology Department, Cairo University, Giza 12613, Egypt

Parker 1982; Abu El Naga 1984; Labib 1984; Schlumberger 1984; unpublished report of Robertson Research International and associates; Kholeif et al. 1986; Barakat et al. 1987, 1988; Abd El-Aal and Moustafa 1988; Nakhla et al. 1992; El Beialy 1995; Schrank and Ibraheim 1995; Ibrahim 1996; Mahmoud and Moawad 2002; Baioumi and Maky 2004; Ibrahim et al. 2009; Zobaa et al. 2011; El Beialy et al. 2010; Aboul Ela and Tahoun 2010; Tahoun 2012; Tahoun et al. 2015; Tahoun and Mohamed 2013, 2020, 2015; Aboul Ela et al. 2018, 2020; Mansour et al. 2020a, 2020b). Most of these studies evaluated source rock characteristics, both qualitatively and quantitatively using traditional TOC/Rock-Eval pyrolysis along with palynofacies and palynomorph microscopy. Recently, Mohamed et al. (2019) presented a detailed palynological study, mainly of the marine-inhabited dinoflagellate cyst and their marker species for biostratigraphic reconstruction of the Santonian-Oligocene interval of the studied Drazia-1 well. This well was drilled in the East Yidma field of the Alamein Basin that is located in the northern part of the Egyptian Western Desert northeast of the Qattara Depression (Fig. 1). In the present work, we deal with the organic content of the syn Syrian Arc deposits (Khoman, Appolonia, and Dabaa formations) to discuss the relationship of the tectonic activities in the region with palynofacies change in addition to the economic importance of the study interval in the giant Alamein Basin. Therefore, we focus on a detailed microscopy through optical analysis to determine palynofacies types and the distribution of the sedimentary organic matter (SOM) in the three formations of the Drazia-1 well. Additionally, detailed characterization of hydrocarbon potential, based on TOC/Rock-Eval pyrolysis, was carried out along with the determination of Kerogen types and thermal maturity levels of the studied rock units. Generally, Alamein, Yidma, Agar, Razzak, and Horus oil fields of the Qattara–Alamein ridge are produced primarily from the Aptian Alamein dolomite and from the Cenomanian Bahariya and Abu Roash "G" reservoirs.

Sedimentary organic matter (SOM) analysis has been effectively employed to offer valuable source rock information when compared to the expensive instrumental geochemical analyses such as Rock-Eval pyrolysis, vitrinite reflectance (R_o%), and gas chromatography-mass spectrometry (cf. Zobaa et al. 2011; Deaf and Tahoun 2018; Aboul Ela et al. 2018; Tahoun et al. 2018; Gentzis et al. 2018a, 2018b; Deaf et al. 2020; Mansour et al. 2020c, 2020d). Tyson (1995) defined the palynofacies analysis as the palynological study of the depositional environments and hydrocarbon source rock prospective relied upon the overall assemblage of particulate organic matter. Moreover, palynofacies analysis can be useful in the interpretation of the tectonic activity in sedimentary basin, since it can distinguish the proximal-distal source of organic matter. The petroleum geochemistry is an applied science for the determination of productive and non-productive zones and properties of source rocks, oil migration, development of oil fields, and continuous production (El Nady et al. 2015).

Geological setting

Drazia-1 well is located in East Yidma Oil Field of Alamein Basin, north western Egypt (latitude 30° 48′ 38.1″ N and a longitude 28° 57′ 37.3″ E). Stratigraphically, it includes three rock units: (1) the Khoman formation that is characterized by open marine deposits and composed of two main units—the lower unit is frequently massive dolomitic limestone with brownish-gray shale interbeds and unconformably overlies the Abu-Roash formation, mainly in the structurally higher area (Mahsoub et al. 2012). The upper unit is described as a white fine-grained, dolomite, and chalky massive limestone intercalated with chert bands (Fig. 2) with poor reservoir properties (Mahsoub et al. 2012). In the Drazia-1 well, Khoman formation extends in depth from 5990 to 5060 ft and ranges in age from Santonian to Maastrichtian (Mohamed et al. 2019). (2) The Apollonia formation consisted of white chalky limestone with minor shale. It overlies the Khoman formation and ranges in age from Paleocene to Middle Eocene (Mohamed et al. 2019). It extends over a depth interval from 5060 to 4710 ft (Fig. 2). (3) The Dabaa formation is consisted of greenish-gray shale, mostly ferruginous in its lower part. It covers the depth interval from 4710 to 3444 ft. This rock unit struggles from late Eocene to Oligocene (Mahsoub et al. 2012; Mohamed et al. 2019, Fig. 2).

In the Alamein Basin, the first Syrian-Arc inversion event took place in the Abu Roash formation, producing folds and faults, and uplifting structures. In the cores of the inversion anticlines, the Santonian and older rock units were completely eroded. The Khoman formation deposited in Tectonosequence 3 (syn-inversion) as a result of the main phase of transgression which commenced in the Campanian and led to high sea levels in the Maastrichtian. (Yousef et al. 2019). The Khoman unit thins above the crests of the hanging-wall inversion anticline structures, but illustrates remarkable thickness variations in the region of the inversion structures, demonstrating that inversion took place during the time of deposition. The Paleocene-Oligocene Apollonia and Dabaa rock units were deposited in the Tectonosequence 4 (late syn-inversion), due to compressional and persistence of the Late Cretaceous folding event which led to onlap at its margins, but with a magnitude less than that of Tectonosequence 3 (Yousef et al. 2009, 2019). The third tectonic event (Syrian Arc event) through the Late Cretaceous to Eocene age inverted several basins of the Western Desert and significantly ended generation and petroleum migration in many areas by the Early Oligocene time, which caused the cessation of hydrocarbon migration from deeper Cretaceous and Jurassic source rocks (Sedek and Al Mahdy 2012).

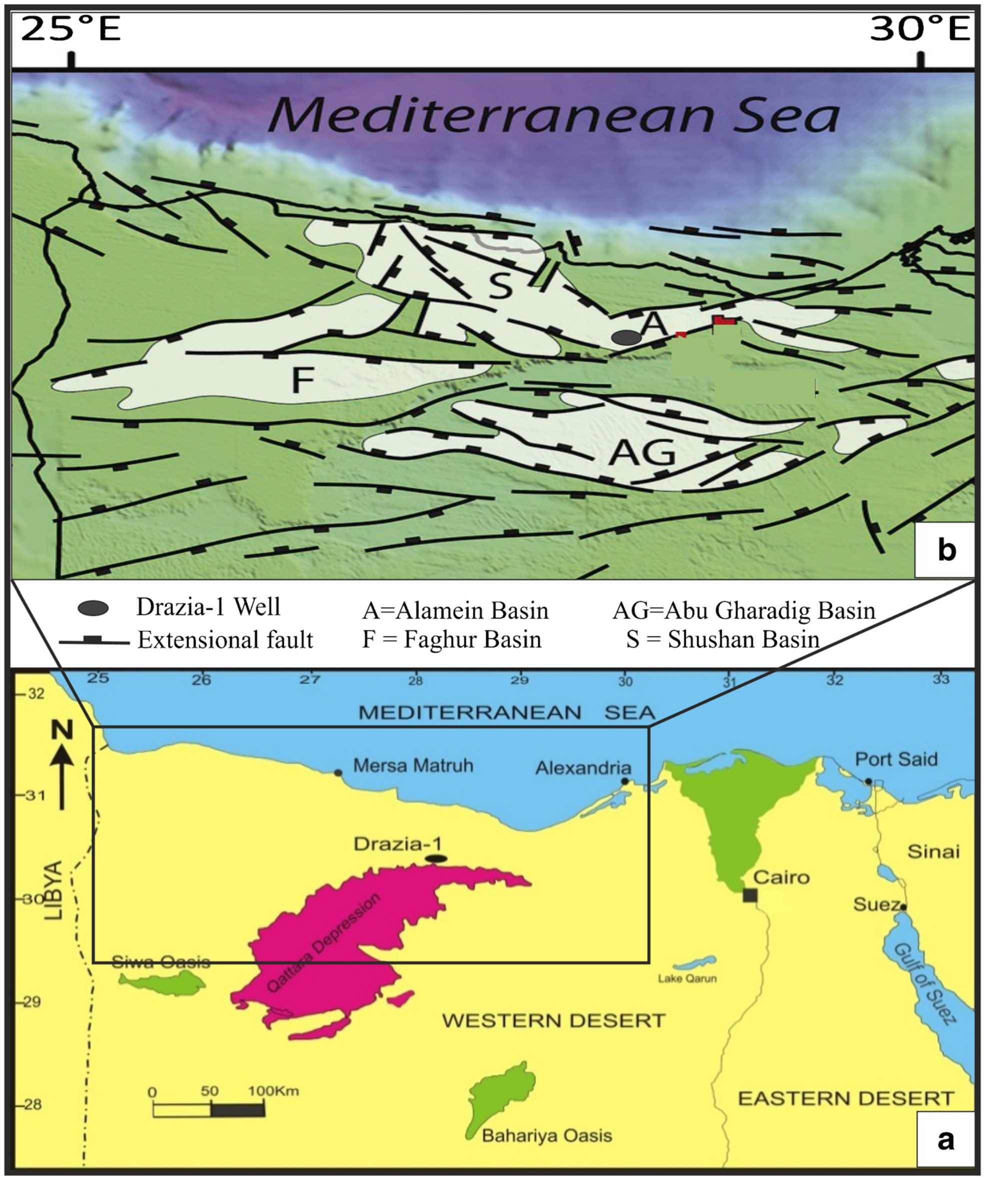

Fig. 1 (A) Location map of the studied Drazia-1 well in the Alamein Basin and (B) the tectonic setting map of the study area in the context of the main Mesozoic and Early Cenozoic basins (white) of Egypt modified after Yousef et al. (2019)

Materials and methods

Palynofacies analysis

A total of 59 cutting samples were recovered from the Drazia-1 well drilled in the East Yidma oil field by the Ina Naftaplin Company in March 2006. About 10–15 g was subjected to routine palynological extraction techniques (Batten 1999). All microscope slides and residues were kept in the Geology Department, Minia University, Egypt. In the present work, a total of 1000 particles per sample were counted and classified according to Tyson (1993, 1995) into three main groups: palynomorphs group (i.e., spores, pollen grains, dinoflagellate cysts, achritarchs, foraminiferal test linings, and fresh water algae), phytoclasts group (i.e., opaque and semi-opaque plus translucent woody particles), and AOM group (i.e., AOM and resin). These groups are illustrated in Tables 1 and 2. To statistically represent the counted data, a cluster analysis of samples was constructed using the statistical program (Past program of Hammer et al. 2001) to characterize the studied succession of the Drazia-1 well into distinctive palynofacies assemblages (Fig. 3a). The counted samples were then plotted on the ternary diagram of Tyson (1993), which comprises the three kerogen-end members AOM, phytoclasts, and palynomorphs (Fig. 3b).

Total organic carbon (TOC) and $CaCO_3$

Good oil-prone source rocks are one of the three major total petroleum system elements, besides intensive reservoirs and excellent seals. Among the critical aspects for

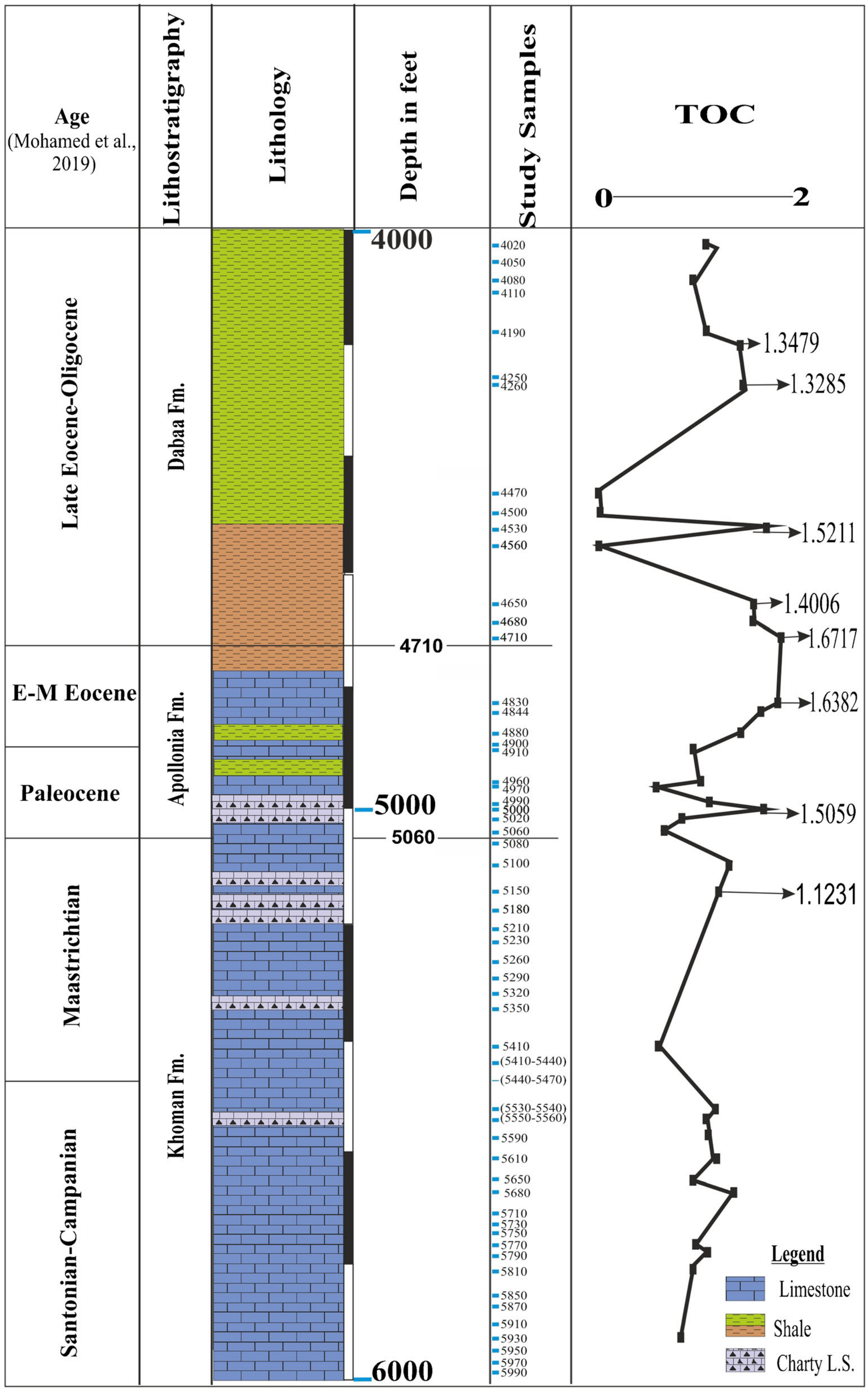

Fig. 2 Lithostratigraphic column of the studied formation and the TOC content in the Drazia-1 well, Western Desert

source rock studies are the quantities of organic matter accumulated throughout deposition and alterations of the post depositional digenesis, and thermal maturation degree (Peters 1986; Peters and Cassa 1994).

For an interval to be a source rock of hydrocarbon generation, it should contain not only appropriate amounts of organic matter, but also the S_2 values that represent the amount of hydrocarbons that might be produced if thermal maturation

Table 1 Quantitative distribution of the palynofacies categories in the Drazia-1 well (depth of 4020–4990 ft), Western Desert

Age			L Eocene-Oligocene													E-M Eocene					Paleocene			
Formation			Dabaa formation														Apollonia fm.							
SOM/sample number			4020	4050	4080	4110	4190	4250	4260	4470	4500	4530	4560	4650	4680	4710	4830	4844	4880	4900	4910	4960	4970	4990
Phytoclasts	Opaque	Equidimensional (O-Eq). Black particle from wood material. Long axis less than twice the short axis. Without internal biostructures.	10	5	7	4	4	8	3	3	9	7	0	2	1	2	3	0	2	3	3	1	1	2
		Lath (O-La). Black particle from wood material. Long axis more than twice the short axis. Without internal biostructures.	40	20	13	44	45	28	22	32	23	40	36	83	13	19	12	2	6	7	4	2	2	3
	Translucent	Wood tracheid with pits (Wp). Brown particle from wood tracheid with visible pits.	0	0	0	0	2	0	0	1	2	0	0	0	1	0	0	0	0	0	2	2	0	1
		Wood tracheid without pits (Ww). Brown particle from wood tracheid without visible pits.	875	899	917	912	911	932	788	909	708	703	613	634	817	847	886	160	904	162	893	963	866	649
		Cuticle (Cu). Thin cellular sheets, epidermal tissue, in some case with visible stomates	3	4	2	2	1	1	0	0	1	0	0	0	0	0	0	0	0	0	0	0	0	0
		Membranes (Mb). Thin, non-cellular, transparent sheets of probable plant origin.	7	0	11	1	1	2	2	1	3	0	2	0	0	0	0	1	0	1	6	4	0	0
		Fungal hyphae (Fh). Individual filaments of mycelium of vegetative phase of eumycote fungi.	1	0	0	0	0	0	0	0	0	0	0	0	0	0	0	0	1	0	2	0	1	0
AOM		AOM. Structureless material. Color: yellow-orange-red;	11	29	10	13	15	9	166	15	217	210	295	238	128	125	90	834	95	796	65	11	113	330

Table 1 (continued)

Age		L Eocene-Oligocene													E-M Eocene					Paleocene			
	orange-brown; gray. Heterogeneity: homogeneous; with "speckles"; clotted; with inclusions (palynomorphs, phytoclasts, pyrite. Form: flat; irregular; angular; pelletal (rounded elongated/oval shape).																						
	Resin. Structureless particle, hyaline, homogeneous, non-fluorescent, rounded, sharp to diffuse outline.	28	28	11	9	8	7	12	17	32	32	38	25	25	25	11	5	4	28	17	10	8	6
Palynomorphs	Spores	8	5	8	5	3	2	2	2	2	2	4	0	4	1	1	2	5	4	1	5	0	2
	Pollen	15	10	14	12	6	6	5	7	5	5	6	2	5	2	3	5	5	3	4	5	1	5
	Dinocysts	1	2	4	3	12	2	6	11	15	3	8	10	21	7	14	10	5	16	17	20	14	11
	Acritarch	1	1	3	4	1	4	1	2	2	0	1	1	1	0	0	0	0	0	0	0	1	0
	Foraminifera test lining	3	0	1	0	1	0	0	6	4	3	3	8	3	4	1	0	0	0	3	1	0	1
	Fresh water algae	0	1	2	1	1	1	1	1	2	0	1	0	4	0	0	0	0	0	0	0	0	0
Total		1003	1004	1003	1010	1011	1002	1008	1007	1025	1005	1007	1003	1023	1032	1021	1019	1027	1020	1017	1024	1007	1010

Table 2 Quantitative distribution of the palynofacies categories in the Drazia-1 well (depth of 5000–5990 ft), Western Desert

Age			Maastrichtian																Santonian-Campanian
Formation			Apollonia fm.					Khoman fm.											
SOM/sample number			5000	5020	5060	5080	5100	5150	5180	5210	5230	5260	5290	5320	5350	5410	(5410_54-40)	(5440_54-70)	(5530_5540)
Phytoclasts	Opaque	Equidimensional (O-Eq). Black particle from wood material. Long axis less than twice the short axis. Without internal biostructures.	0	0	0	0	0	0	1	0	1	1	0	7	1	0	2	0	0
		Lath (O-La). Black particle from wood material. Long axis more than twice the short axis. Without internal biostructures.	0	3	2	3	1	2	2	0	2	3	0	23	0	0	15	1	1
	Translucent	Wood tracheid with pits (Wp). Brown particle from wood tracheid with visible pits.	1	1	0	0	0	0	0	1	1	2	4	38	7	1	2	1	0
		Wood tracheid without pits (Ww). Brown particle from wood tracheid without visible pits.	84	76	83	87	165	97	128	267	123	98	121	98	65	121	400	168	73
		Cuticle (Cu). Thin cellular sheets, epidermal tissue, in some case with visible stomates.	0	0	0	0	0	0	0	1	0	0	0	0	0	0	1	0	1
		Membranes (Mb). Thin, non-cellular, transparent sheets of probable plant origin.	0	0	0	1	2	0	0	1	3	1	0	0	0	0	3	4	0
		Fungal hyphae (Fh). Individual filaments of mycelium of vegetative phase of eumycote fungi.	0	0	0	1	0	1	2	0	0	0	1	0	0	0	0	0	0
AOM		AOM. Structureless material. Color: yellow-orange-red; orange-brown; gray. Heterogeneity: homogeneous; with “speckles”; clotted; with inclusions (palynomorphs, phytoclasts, pyrite. Form: flat; irregular; angular; pelletal (rounded elongated/oval shape).	890	872	873	880	805	839	734	680	826	872	861	761	906	845	566	797	887
		Resin. Structureless particle, hyaline, homogeneous, non-fluorescent, rounded, sharp to diffuse outline.	4	4	3	4	6	5	12	4	6	14	3	7	8	7	12	11	9
Palynomorphs		Spores	0	1	1	2	3	2	5	0	1	1	0	0	0	1	1	1	2
		Pollen	2	5	3	2	5	7	9	9	5	4	5	2	3	2	2	1	4
		Dinocysts	22	50	44	26	27	52	112	54	45	25	11	64	18	41	11	28	23
		Acritarch	0	1	0	0	0	0	0	0	0	0	1	1	0	0	0	0	0
		Foraminifera test lining	0	2	1	3	2	3	9	7	1	0	0	3	0	0	1	0	0
		Fresh water algaa	0	0	0	0	0	0	1	0	0	0	1	0	0	0	0	1	2
Total			1003	1015	1010	1009	1016	1008	1015	1024	1014	1021	1008	1004	1008	1018	1016	1013	1002

Age	Santonian-Campanian
Formation	Khoman fm.

Table 2 (continued)

SOM/sample number	(5550_ 5560)	(5570_ 5580)	(5590_ 5600)	(5610_ 5620	5650	(5660_ 5670)	(5680_ 5690)	5710	5730	5750	5770	5790	5810	5850	5870	5910	5930	5950	5970	5990
Phytoclasts	0	1	1	0	0	4	0	0	0	1	0	0	0	1	0	0	0	0	0	0
	0	4	6	4	2	5	0	3	1	1	0	0	2	1	0	0	1	0	1	2
	0	1	0	0	0	2	0	0	1	0	0	1	1	6	3	3	12	7	2	2
	106	132	193	182	193	590	196	138	306	153	132	98	78	107	111	74	87	85	67	97
	0	0	0	0	0	0	0	0	0	0	0	0	0	0	0	0	0	0	0	0
	1	0	1	1	0	3	0	1	0	0	1	0	0	0	0	1	0	0	1	0
	0	0	0	0	1	0	0	1	0	0	0	0	0	0	0	0	0	0	0	0
AOM	873	809	771	777	748	312	760	792	593	816	798	873	898	882	863	919	875	867	916	896
	9	15	13	16	10	19	3	10	11	13	12	2	8	1	3	5	2	1	0	0
Palynomorphs	1	2	1	2	2	3	3	2	2	2	3	1	1	0	1	0	1	0	0	2
	3	3	2	3	2	4	8	7	5	5	7	3	5	1	3	1	4	2	2	2
	20	32	15	22	41	61	35	56	85	28	59	24	14	12	20	22	23	45	11	5
	0	1	0	0	0	1	1	4	1	1	0	0	0	0	0	0	0	0	0	0
	0	1	1	0	3	5	3	3	5	3	4	4	0	4	1	2	0	0	0	2
	0	0	1	0	0	0	0	0	0	0	0	0	0	0	0	0	0	0	0	0
Total	1013	1001	1005	1007	1002	1009	1009	1017	1010	1023	1016	1006	1007	1015	1005	1027	1005	1007	1000	1008

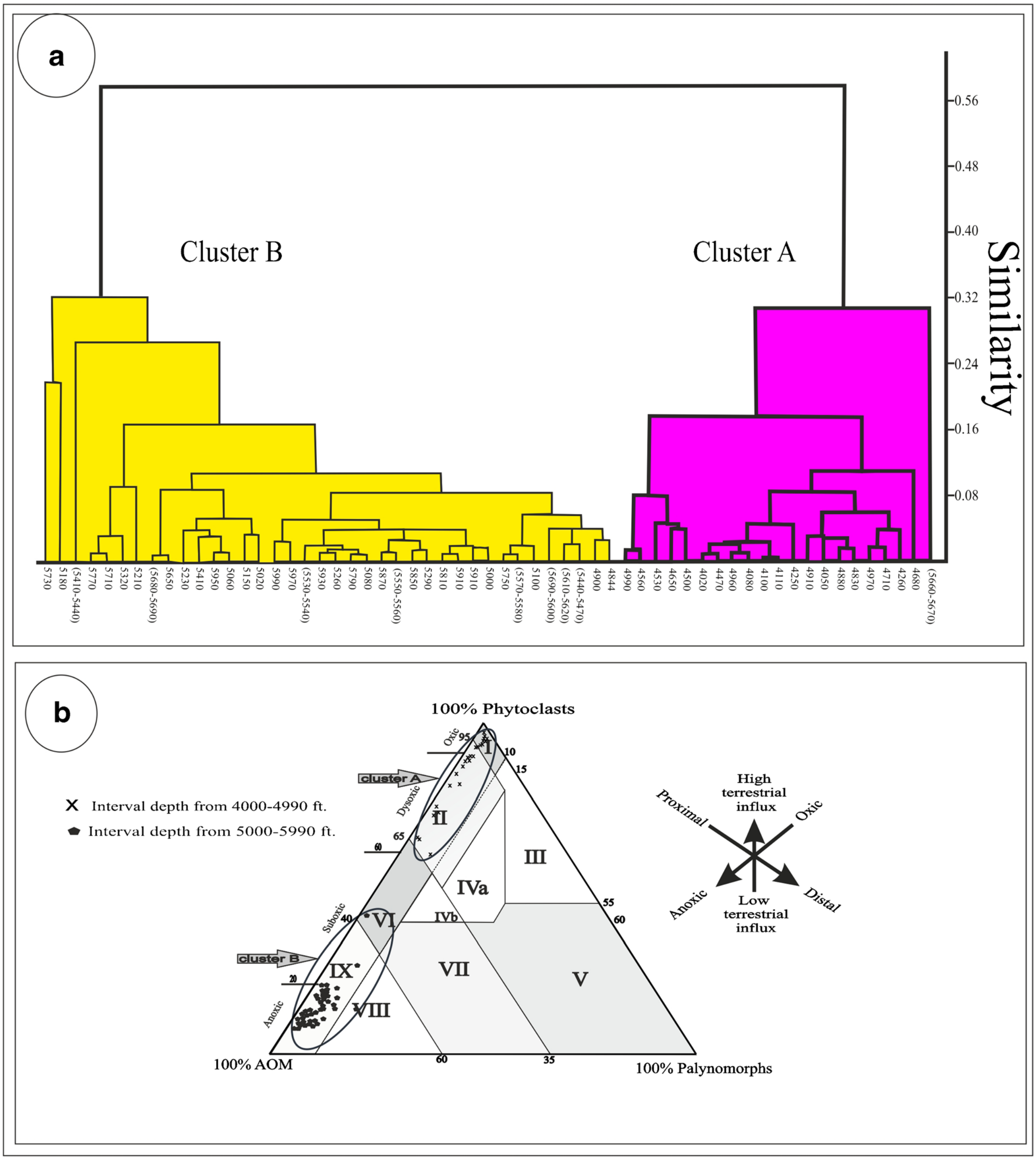

Fig. 3 **a** Cluster analysis of the studied samples in the Khoman, Apollonia, and Dabaa formations; cluster A is phytoclast-AOM assemblage and cluster B is AOM assemblage. **b** AOM-palynomorph-phytoclast ternary plot (after Tyson 1993) of the relative numerical particle frequency (% of the total POM content) in Drazia-1 well, Western Desert, Egypt

continues (Batten 1996). In the present study, thirty-nine samples were measured for their TOC using a LECO C230 carbon analyzer (Table 3) and carried out in the Department of Geodynamics and Sedimentology, University of Vienna. The carbonate content ($CaCO_3$) was calculated using the formula

$$CaCO3 = \text{inorganic carbon} \times 8.333.$$

The minimum values that were taken for a probable source rock interval was 0.5 wt% TOC as a cutoff for fine clastics and shales and around 0.3 wt% for carbonates (e.g., Hedberg et al. 1979). Peters (1986) rated a content of TOC < 0.5 wt% as poor, 0.5–1 fair, 1–2 good, and greater than 2.0 very good, whereas Peters and Cassa (1994) noted that a minimum organic carbon content of a source rock should be within the range of 1–2 wt%.

Rock-Eval pyrolysis

Valuable information concerning the quantity, quality (type), and thermal maturity of the organic matter in a sedimentary rock can be provided by the Rock-Eval pyrolysis data (Espitalie et al. 1977. After the primary TOC showing, all samples measuring over than 1.5 wt% TOC were selected

Table 3 The TOC measurements in Drazia-1 well in Western Desert

Age (after Mohamed et al. 2019)	Formation	Sample no.	TOC (%)	TIC (%)	TC (%)
Late Eocene - Oligocene	Dabaa formation	4020	1.0837	0.0583	1.1420
		4080	0.9338	0.0490	0.9828
		4190	1.0693	0.2244	1.2937
		4200	1.3479	0.9203	2.2682
		4260	1.3285	0.7340	2.0625
		4410	0.8663	0.0326	0.8989
		4440	1.5009	0.4012	1.9021
		4530	1.5211	0.3239	1.8450
		4620	1.6956	0.3514	2.0470
		4650	1.4006	0.5198	1.9204
		4680	1.4102	0.8145	2.2247
E-M Eocene		4710	1.6717	0.9039	2.5756
	Apollonia formation	4830	1.6382	2.4327	4.0708
		4844	1.4800	0.8515	2.3314
		4880	1.3103	4.0428	5.3531
Paleocene		4910	0.9462	6.7095	7.6556
		4960	0.9874	6.0217	7.0091
		4970	0.6615	8.0736	8.7351
		4990	1.0786	3.6046	4.6832
		5000	1.5059	5.4356	6.9416
		5020	0.8611	4.1480	5.0091
		5060	0.6932	7.0574	7.7506
Maastrichtian	Khoman formation	5100	1.2185	3.5854	4.8039
		5130	0.9491	4.8351	5.7842
		5150	1.1231	4.7900	5.9131
		5410	0.6754	5.5442	6.2196
		5440	0.6496	6.8523	7.5019
Santonian-Campanian		5500	0.8748	4.7561	5.6309
		5530–5540	1.0938	4.6844	5.7782
		5550–5560	1.0841	4.1926	5.2767
		5590	1.0196	5.0856	6.1051
		5610	1.1073	4.8602	5.9675
		5650	0.9537	5.4244	6.3781
		5660	0.9835	5.4009	6.3844
		5680	0.9309	5.7604	6.6913
		5770	0.9737	5.2159	6.1896
		5790	1.0053	4.4117	5.4170
		5810	0.9313	5.7956	6.7269
		5930	0.8215	7.1875	8.0090

for the Rock-Eval pyrolysis in 10 distinct intervals (Table 3). Rock-Eval pyrolysis comprises passing a stream of helium through 100 mg of crushed rock heated firstly at 300 °C followed by heating at 25 °C/min to 550 °C. The vapors are analyzed with a flame ionization detector (FID) and the emitted CO_2 by heating at 390 °C and is measured by thermal conductivity detector (TCD). The resulting parameters comprise S_1 (free hydrocarbons), S_2 (hydrocarbon yield from thermal cracking of kerogen), S_3 (the trapped CO_2 freed during pyrolysis), and T_{max} (Rock-Eval pyrolysis oven temperature °C at maximum S_2 generation). Hydrogen index (HI) is a calculated parameter based mainly on the measured TOC and S_2 values [HI = (S_2/TOC) × 100, mg HC/g TOC]. Oxygen index is also a calculated parameter from the formula [OI = (S_3/TOC) × 100, mg CO_2/g TOC]. Production index is the ratio between the released free hydrocarbons (S_1) and total hydrocarbons of thermal cracking ($S_1 + S_2$), pyrolyzable carbon index; [PCI = 0.83 × ($S_1 + S_2$)] and S_2/S_3 together with HI are relative to the quantity of hydrogen in the kerogen and can designate the potential of the rock to generate oil (Hunt 1996). The measured values of samples by the Rock-Eval pyrolysis are summarized in Table 4.

Results

Palynofacies assemblages

A palynofacies is defined as the complete assemblage of organic matter and palynomorphs in a fossil deposit. Palynofacies analysis includes the incorporated study of the entire aspects of the organic matter assemblage, which includes the recognition of the individual particulate components, estimation of their relative and absolute proportions, and their size and preservation states (Combaz 1980).

The palynofacies analysis in the Drazia-1 well reflects a high abundance of AOM in the Upper Cretaceous succession compared to high concentration of brown and black phytoclasts in the Paleocene-Oligocene interval (Tables 1 and 2).

The statistical analysis based on the ratio of sedimentary organic material groups (palynomorphs, phytoclasts, and AOM) encountered through the three formations enabled us to differentiate two palynofacies assemblages based on cluster analysis into clusters A and B using the Ward's method of the PAST program (Fig. 3a). Moreover, all samples were plotted on the AOM-phytoclasts-palynomorphs ternary diagram after Tyson (1993) in order to interpret their depositional environments (Fig. 3b).

Palynofacies type 1 (PF1) assemblage was proposed to cluster A and was dominated by phytoclasts and AOM. It is the dominant palynofacies assemblage in the studied samples and covers the Dabaa and Apollonia formations. It is represented by 21 samples in the Drazia-1 well and ranges from 4020 to 4990 ft, except for two samples at depths of 4844 and 4900 ft. This cluster is typified by a relatively high abundance of phytoclasts (65.5–97.2%) compared to low to high abundance of AOM (9–83%) and low palynomorph content (13–38%) mainly the terrestrial pollen grains and spores but the marine dinoflagellate cysts and acritarchs are very rare in this assemblage (Figs. 3b, 4a, b). The maximum phytoclast content is recognized in sample at a depth of 4960 ft, while the minimum content is observed at a depth of 4990 ft. The phytoclasts are dominated by brown particles of wood tracheid without visible pits as opposed to moderate to low content of black wood debris.

According to the ternary diagram of Tyson (1993), all samples of this cluster plot in the palynofacies fields I and II, which reflect deposition in a highly proximal shelf environment or basin and marginal oxic-dysoxic basin conditions, respectively (Fig. 4a, b). Additionally, these fields indicate kerogen type III of gas-prone hydrocarbons.

Palynofacies type 2 (PF2) assemblage was assigned to samples of cluster B and is considered the dominant palynofacies assemblage in the studied Khoman formation. This palynofacies includes 37 samples and ranges from 5000 to 5990 ft, except for a sample at depth of 5660–5670 ft. This palynofacies assemblage of cluster B is characterized by a relatively high abundance of AOM (74.6–92.4%); however, the sample depth 5660–5670 ft contains a relatively low AOM content (33.1%, Figs. 3b, 4c, d).

Most of the samples of the second palynofacies assemblage plot in the field IX of Tyson (1993), except for one sample that has a relatively high palynomorph content and plot in the palynofacies field VI. Additionally, one more sample plot in the palynofacies field VIII (Fig. 3b). According to Tyson (1993, 1995), the palynofacies field IX indicates deposition of samples in a distal suboxic-anoxic basin with low

Table 4 Guidelines for pyrolysis parameters of quality, quantity, and thermal maturity in Drazia-1 well, Western Desert (adapted and modified after both Tyson (1995) and Peters and Cassa (1994))

Depth	Formation	TOC	S1	S2	GP	S3	Tmax	HI	OI	PI
4200	Dabaa	1.3479	0.11	0.76	0.87	4.68	421	56.38	347.21	0.13
4260		1.3285	0.08	0.66	0.74	4.06	423	49.68	305.61	0.11
4440		1.5009	0.10	0.93	1.03	3.70	420	61.96	246.52	0.10
4530		1.5211	0.09	1.01	1.1	3.95	424	66.4	259.68	0.08
4620		1.6956	0.11	1.04	1.15	3.74	421	61.34	220.57	0.10
4650		1.4006	0.15	1.27	1.42	5.07	427	90.68	361.99	0.11
4710		1.6717	0.14	1.16	1.3	4.64	424	69.39	277.56	0.11
4830	Apollonia	1.6382	0.13	1.21	1.34	4.32	427	73.86	263.7	0.10
5000		1.5059	0.19	1.36	1.55	3.73	429	90.31	247.69	0.12
5150	Khoman	1.1231	0.11	0.76	0.87	3.10	424	67.67	276.02	0.13

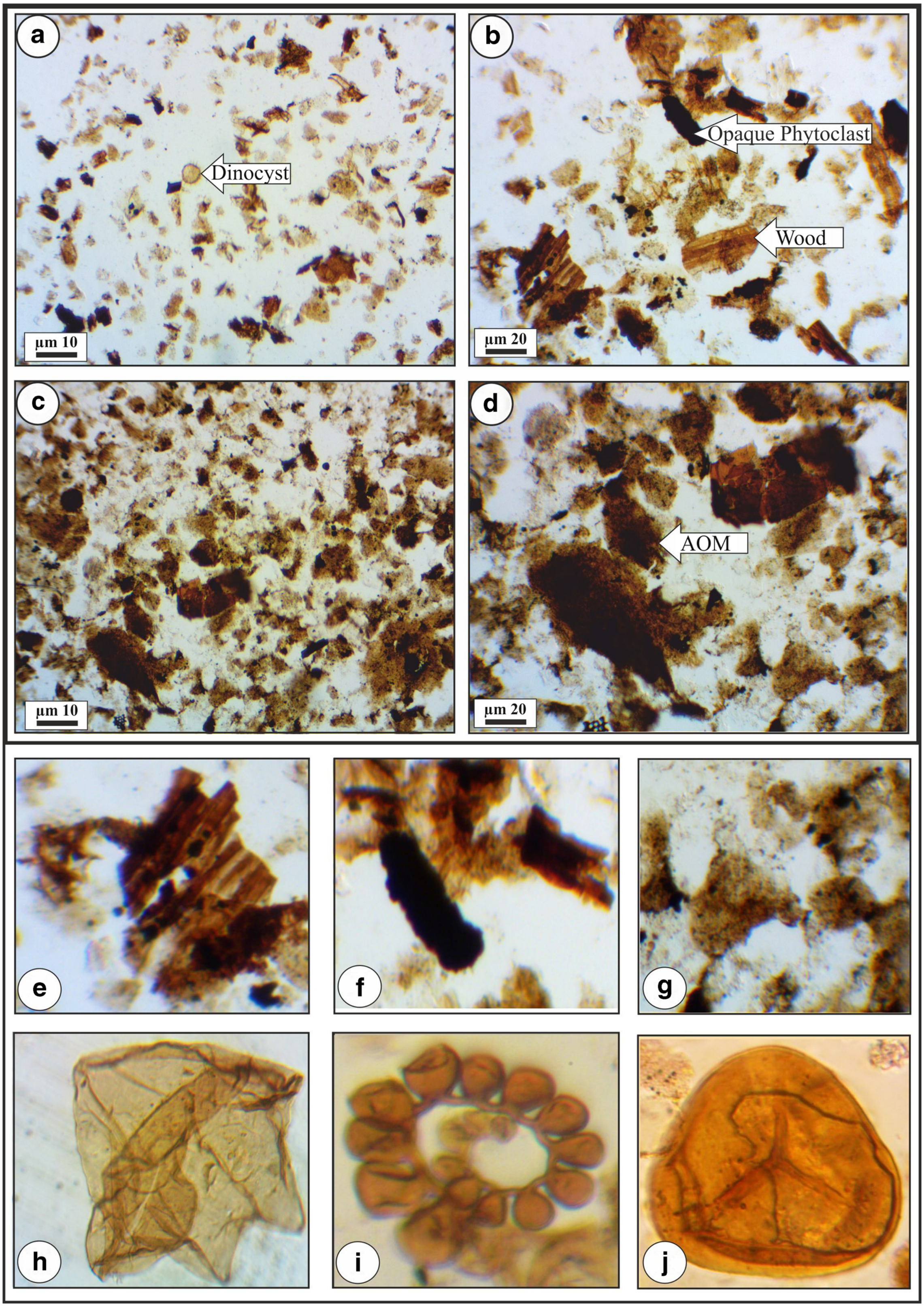

Fig. 4 **a**, **b** The first palynofacies assemblage that composed mainly of phytoclasts-AOM; the photomicrographs were recovered from the depth interval of 4190 ft in Drazia-1 well. **c**, **d** The second palynofacies assemblage that is dominated by the AOM recovered from the sample at a depth of 5930 ft in Drazia-1 well. **e** Brown wood particles, **f** lath black phytoclast, **g** AOM, **h** dinoflagellate cyst, **i** foraminifera lining, **k** spores

abundance of palynomorphs possibly owing to masking, regularly alginate-rich, deep basin, or stratified shelf-sea sediments, especially sediment-starved basins. Besides, samples of this assemblage contain oil-prone kerogen type II.

Source rock evaluation

The assessment of source rocks in the studied well is based upon the pyrolysis parameters like TOC, S_1, S_2, HI, OI, T_{max}, and VR which provide significant information for petroleum generation potential and characterization (e.g., Peters and Cassa 1994; Tahoun et al. 2018; Gentzis et al. 2018a, 2018b; Deaf et al. 2020; Mansour et al., 2020 b, c). Additionally, common plots such as the modified van Krevelen diagram, the HI versus T_{max} plot, T_{max} versus PI, and TOC versus S_1+S_2 diagrams are integrally used to further confirm the potentiality of probable source rock layers and to define the type of produced hydrocarbon and their thermal maturity levels.

Hydrocarbon potential

Peters and Cassa (1994) accounted for measuring the amount of TOC and S_2 to evaluate the quantity of organic matter in the studied formations. They revealed that "the samples which have TOC less than 0.5 wt% and S2 less than 2.5 mg/g are considered poor source rocks. Samples contain TOC from 0.5 to 1.0 wt % and S2 from 2.5 to 5 mg/g are fair source rocks. Samples contain TOC from 1 to 2 wt % and S2 from 5 to 10 mg/g are good source rocks and samples that contain more than 2 wt % TOC and S2 > 10 mg/g are considered very good source rocks". In the present study, the selected samples for Rock-Eval pyrolysis analyses have high TOC content which is good and ranges from 1.1 to 1.7 wt%. The S2 values ranges between 0.66 and 1.36 mg HC/g rock (Table 4), indicating a poor hydrocarbon generating potential and accordingly a poor source rocks in the Khoman, Apollonia, and Dabaa formations. The hydrocarbon generation prospective of a source rock is the sum of the values S_1 and S_2 (Peters and Cassa 1994). According to Hunt (1996) and Gogoi et al., (2008), the source rocks with a generation potential of < 2 are considered poor, 2–5 fair, 5–10 good, and > 10 very good (Fig. 5). Based on the plot between S_1+S_2 and TOC, the Khoman, Apollonia, and Dabaa formations have a poor hydrocarbon generation potential (Fig. 5, Table 4).

Type of kerogen

The type of organic matter is a significant factor in assessing the source rock potential and has vital control on the nature of the hydrocarbon yields (Hunt 1979; Tissot and Welte 1984; Barker 1996). From the Rock-Eval pyrolysis data, such as HI, various types of organic matter kerogens can be recognized

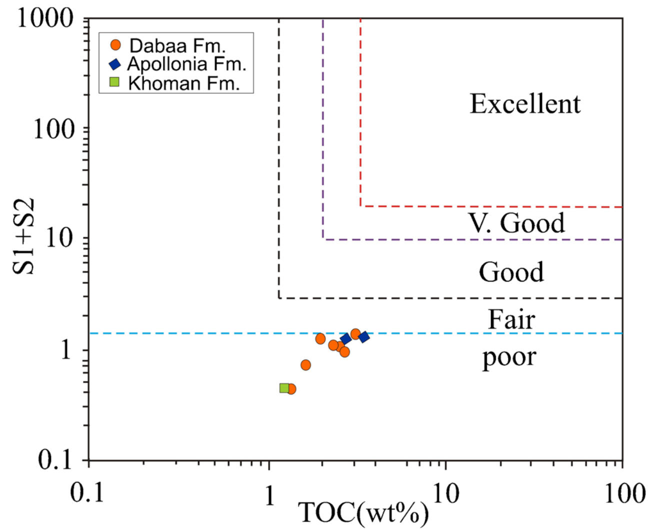

Fig. 5 The generation potential of the studied source rocks as indicated by the relationships between TOC and S1 + S2 (after Gogoi et al. 2008) in Drazia-1 well, Western Desert

(Waples 1985). HI values that are less than 200 mg HC/g TOC point to a possible source for gas generating (mostly type III kerogen), whereas HI ranging between 200 and 300 mg HC/g TOC contains a mixed kerogen type III/II, and as a result is capable of producing mixed gas and oil (Peters and Cassa 1994).

The investigated samples in Drazia-1 well have low HI values that range from 49.7 to 90.7 mg HC/g TOC, though OI values range from 220.6 to 362 mgCO_2/g TOC (Table 4). The HI values usually lie in a typical range of kerogen type III of terrestrial organic matter (e.g., Peters and Cassa 1994; Mansour et al. 2020c). These results are further confirmed

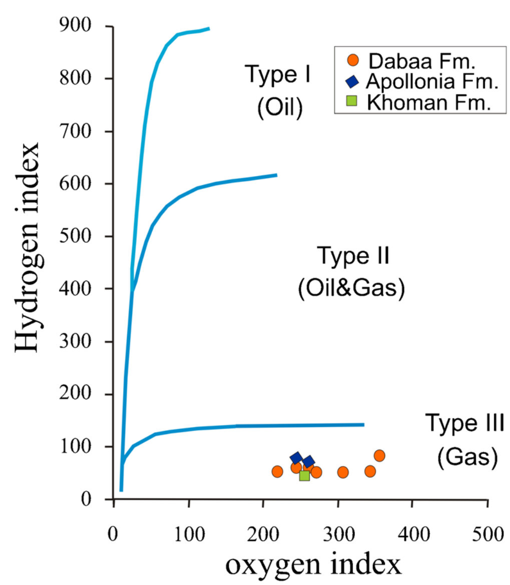

Fig. 6 HI versus OI of the modified Van Krevelen diagram (after Van Krevelen 1993), showing the type of kerogen in the Drazia-1 well, East Yidma field

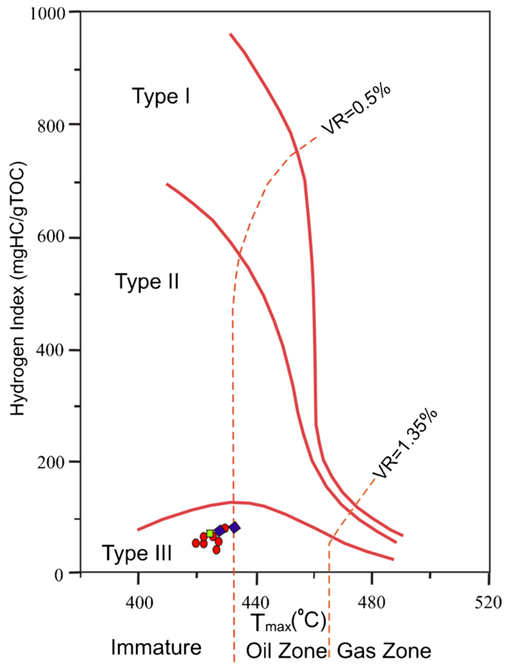

Fig. 7 HI versus T_{max} plot (after Koeverdon et al. 2011), showing the maturity and type of Kerogen in the analyzed samples of the Drazia-1 well, East Yidma field

by the Van Krevelen diagram (Van Krevelen 1993), whereby all samples plot in the fields of type III to IV kerogens (Fig. 6). Additionally, the HI versus T_{max} plot for the studied samples in the Drazia-1 well indicates mainly a kerogen type III of terrestrial woody material typically of gas-prone hydrocarbons (Fig. 7).

Thermal maturity

Source rock maturity of the studied samples is estimated from the T_{max} and production index "PI values." Many maturity parameters, especially T_{max}, based on the type of organic matter, from which they derived (Peters 1986). It was stated that oil generation from source rocks started at T_{max} of *ca*. 435 °C that gradually increases in thermal maturity levels to 465 °C at peak of gas generation (e.g., Peters and Cassa 1994). These values are consistent with the PI values, which commonly range between 0.2 and 0.4.Therefore, the organic matter are in the immature stage for a PI value of less than 0.2, whereas the gas window is consistent with a PI value of more than 0.4 (e.g., Peters and Cassa 1994).

For the studied formations, the pyrolysis T_{max} values (Table 4) are below 435 °C, representing that the source rocks are still in the immature stage. The maturity estimates from the HI versus T_{max} plot also showed the same maturity level, whereby all samples were in the immature stage. Furthermore, the PI values for the Khoman, Apollonia, and Dabaa formations range from 0.08 to 0.13 in agreement with the T_{max} results, which reinforce an immature stage (Fig. 8).

Discussion

The palynofacies analysis in the Drazia-1 well reflects two different marine environments. The relatively deeper one which is characterized by a high abundance of AOM and carbonate contents were recognized in the Upper Cretaceous succession (Khoman formation). The relatively shallower environment is characterized by a high abundance of phytoclasts and siliciclastic contents in the Paleocene-Oligocene interval (Dabaa and Appolonia formations). The relative changes in the water depth of the Upper Cretaceous and Paleogene may be related to the variations in the region of the inversion structures by the Syrian Arc System which took place during the time of deposition (e.g., Yousef et al. 2009, 2019). Ruban et al. (2010) confirmed that, in the Northeastern Africa, mainly Western Desert, there is a discrepancy between documented

Fig. 8 PI versus T_{max} (°C) showing the thermal maturation levels of the Drazia-1 well, East Yidma field (adopted after GeoMark sheet)

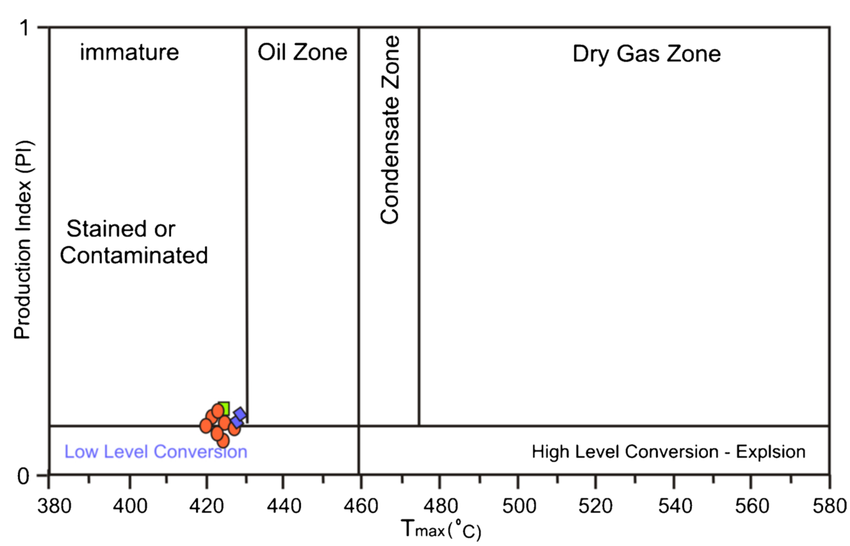

transgression-regression patterns and the eustatic sea level changes in the Paleocene period. The regional subsidence or uplift controlled transgressions and regressions locally. The very low hydrocarbon potential and moderate to low content of organic matter preserved within the studied Khoman and Apollonia formations can be referred to various environmental processes that include carbonate effect during deposition, redox conditions, role of sediment supply, and sedimentation rate (e.g., Mansour et al. 2020a). For this purpose, we plotted the TOC values versus $CaCO_3$ to address the relationship between both variables in the carbonate-rich intervals (Fig. 9). The relationships between TOC versus $CaCO_3$ content were proposed by Ricken (1996). In this model, the $CaCO_3$ content varies and organic matter and siliciclastics were assumed to be constant. In other words, the relative increase in $CaCO_3$ would result in a dilution of accumulated organic carbon content and lead to an overall decrease in the TOC in sediments. For the Khoman and Apollonia formations, a moderate R^2 value (0.48) was observed between the TOC and $CaCO_3$ (Fig. 9), confirming a moderate relationship between both variables during deposition within the Late Cretaceous marine ecosystem (e.g., Mansour et al. 2020a, 2020e). Additionally, the normal distribution between samples in Fig. 9 showed a negative correlation, confirming the proposed hypothesis of Ricken (1996). However, redox conditions and role of sediment supply require more geochemical data to be addressed, providing a recommendation for future studies of such important succession.

The thermal immature stage of the Khoman, Apollonia, and Dabaa formations is thought to be attributed to two main factors, the local to regional tectonic activity and burial thickness of sediments. The northern region of Egypt, including the north Western Desert, Nile Delta, and Sinai Peninsula, has been influenced by several structural processes during the Late Cretaceous to Cenozoic (EGPC (Egyptian General Petroleum Corporation) 1992). This included the Syrian Arc System that initiated from the Turonian-Santonian and reached the main phase of activity during the middle Eocene. Additionally, the other tectonic cycle was represented in the Red Sea opening and Gulf of Suez rifting phase that activated during the Oligocene to Miocene (EGPC (Egyptian General Petroleum Corporation) 1992). Since the studied formations were deposited during the Late Cretaceous to Oligocene, these tectonic activities that influenced northern Egypt are suggested to uplift the sedimentary succession in the studied area. The uplifting consequently reduced the burial depth and led to the immaturity for source rock hydrocarbon.

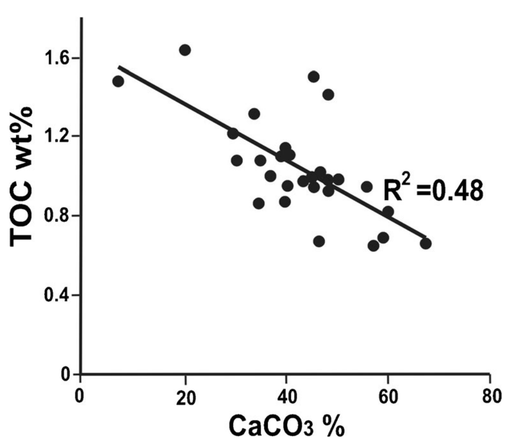

Fig. 9 Plot of TOC versus $CaCO_3$ for carbonate-rich intervals of the Khoman and Apollonia formations to interpret the relationship between both variables during deposition

Conclusion

The palynofacies analysis were carried out on 59 cutting samples. The organic geochemical TOC were conducted on 39 samples and the Rock-Eval pyrolysis was conducted on 10 samples, from the Khoman, Apollonia, and Dabaa rock units in the Drazia-1 well, East Yidma Oil Field, Alamin Basin. Two palynofacies assemblages were proposed for the studied succession. The Paleocene-Oligocene succession was assigned to the first palynofacies assemblage that is typified by a high abundance of brown and black phytoclasts and reinforces deposition in a proximal shelf or basin of gas-prone kerogen type III. A high abundance of AOM in the Upper Cretaceous succession of the second palynofacies assemblage indicates a distal suboxic-anoxic basin of oil-prone kerogen type II. In the Alamien Basin, the palynofacies analysis indicates relatively deeper marine environment in the Upper Cretaceous, since it is characterized by an abundance of marine dinocysts and AOM, and shallower environment in the Paleogene which is characterized by abundance of terrestrial pollen grains, spores, and phytoclasts. This variation is related to the tectonic movements in the northern Egypt, mainly the Syrian Arc System. The local uplifting in the Alamein Basin reduced the burial depth and thermal maturation for organic matter in the Khoman, Apollonia, and Dabaa formations of the Drazia-1 well.

The organic matter content in Khoman, Apollonia, and Dabaa formations of the Drazia-1 well is not potential for those that are gas-prone. Furthermore, the T_{max} and PI values indicated that the Khoman, Apollonia, and Dabaa formations were in the immature stage.

Acknowledgments We express our thanks to Petr Skupien, Faculty of Mining and Geology, VSB-Technical University of Ostrava, and Michael Wagreich, Department of Geodynamics and Sedimentology in Vienna University, for the TOC measurements.

References

Abd El-Aal A, Moustafa AR (1988) Structural framework of the Abu Gharadig Basin, Western Desert, Egypt, Paper presented at the 9th Exploration and Production Conference. Egypt Gen Pet Corp Cairo 2:23–50

Aboul Ela N, Tahoun SS (2010) Dinoflagellate cyst stratigraphy of the subsurface Middle-Upper Jurassic / Lower Cretaceous sequence in North Sinai, Egypt. 5th International Conference on the Geology of the Tethys Realm, South Valley University, January 2010, 85-115.

Aboul Ela N, Tahoun SS, Fouad T, Mousa D, Saleh R (2018) Source rock evaluation of Kharita and Bahariya formations in some wells, north Western Desert, Egypt: visual palynofacies and organic geochemical approaches. Egypt Jof Petrol 27:455–465

Aboul Ela N, Tahoun SS, Raafat A (2020) The Cretaceous (Barremian-Maastrichtian) palynostratigraphy and palynofacies of the Drazia-1 well, north Egypt. Palynology 44(1):94–113

Abu El Naga M (1984) Paleozoic and Mesozoic depocenters and hydrocarbon generating areas, northern Western Desert, Paper presented at the 7th Petroleum and Exploration Seminar. Egypt Gen Pet Corp Cairo 8:269–287

Baioumi AA, Maky AF (2004) Palynostratigraphy, palynofacies and palaeoenviromental interpretation of the Bahariya formation in Salam-IX Well, Western Desert. Egypt J Paleont 4:157–172

Barakat MG, Darwish M, Abdel Hamid ML (1987) Hydrocarbon source rock evaluation of the Upper Cretaceous (Abu Roash Format ion) east Abu Gharadig Area, North Western Desert, Egypt. M. E. R. C. Ain Shams University. Earth Sci Ser 1:120–150

Barakat MG, Darwish M, Ghanem MF (1988) Evolution, sedimentary environments and hydrocarbon potentials of the Kharita formation (Albian) in the North Western Desert, Egypt. Proceedings of EGPC Ninth Petroleum Exploration and Production Conference. EGPC, Cairo 2:5l–73l

Barker C (1996) Thermal modeling of petroleum generation: theory and applications. Elsevier Science & Technology, New York ISBN10: 0444820302

Batten DJ (1996) Palynofacies and petroleum potential. In: Jansonius J, McGregor DC (eds) Palynology: principles and applications, vol 3. American Association of Stratigraphic Palynologists' Foundation, Dallas, pp 1065–1084

Batten DJ (1999) Palynofacies analysis. In: Jones TP, Rowe NP (eds) Fossil plant spores, modern techniques .Geological Society, London, pp 194–198

Combaz A (1980) Les kérogènesvus au microscope. In: Durand B (ed) Kerogen: insoluble organic matter from sedimentary rocks, Edition edn. Technip, Paris, pp 55–111

Deaf AS, Tahoun SS (2018) Integrated palynological, organic geochemical, and sequence stratigraphic analyses of the middle to upper Cenomanian hydrocarbon reservoir/source Abu Roash "G" Member: A depositional model in north western Egypt. Mar Pet Geol 92:372–402

Deaf AS, Tahoun SS, Gentzis T, Carvajal-Ortiz H, Harding IC, Marshall JE, Ocubalidet S (2020) Organic geochemical, palynofacies, and petrographic analyses examining the hydrocarbon potential of the Kharita formation (Albian) in the Matruh Basin, northwestern Egypt. Mar Pet Geol 112:104087

EGPC (Egyptian General Petroleum Corporation), (1992). Western desert, oil and gas fields, a comprehensive overview. In: EGPC 11th Petroleum Exploration and Production Conference, Cairo, 431 pp.

El Beialy SY (1995) Datation and Palaeoenvironmental interpretation by microplankton and miospore assemblages of the Razzak Oil Field sediments, Western Desert, Egypt. Geobios 28:663–673

El Beialy SY, El Atfy HS, Zavada MS, El Khoriby EM, Abu-Zied RH (2010) Palynological, palynofacies, paleoenvironmental and organic geochemical studies on the Upper Cretaceous succession of the GPTSW-7well, North Western Desert, Egypt. Mar Pet Geol 27: 370–385

El Nady MM, Ramadan F, Hammad MM, Lotfy NM (2015) Evaluation of organic matters, hydrocarbon potential and thermal maturity of source rocks based on geochemical and statistical methods: case study of source rocks in Ras Gharib oilfield, central Gulf of Suez, Egypt. Pet Sci 24(2):203–211

Espitalie J, Madec M, Tissot BP, Menning JJ, Leplat P (1977) Source rock characterization method for petroleum exploration. Ninth Ann Offshore Technol Conf Proc 3:439–448

Gentzis T, Carvajal-Ortiz H, Deaf AS, Tahoun SS (2018a) Multi-proxy approach to screen the hydrocarbon potential of the Jurassic succession in the Matruh Basin, North Western Desert, Egypt. Int J Coal Geol 190:29–41

Gentzis T, Carvajal-Ortiz H, Selim SS, Tahoun SS, El-Shafeiy M, Ocubalidet S, Ali AA (2018b) Depositional environment and characteristics of Late Eocene carbonaceous swampy tidal flat facies in the Fayoum Basin, Egypt. Int J Coal Geol 200:45–58

Gogoi K, Dutta MN, Das PK (2008) Source rock potential for hydrocarbon generation of Makum coals, Upper Assam. India J Curr Sci 95: 233–239

Hammer Ø, Harper DAT, Ryan PD (2001) PAST: Paleontological Statistics Software Package for Education and data analysis. Palaeontol Electron 4(1):9

Hantar G, 1990. Northern Westem Desert. In: Said R (ed) The geology of Egypt, 293-319 pp.

Hedberg HD, Moody JD, Hedberg FLM (1979) Petroleum prospects of deep offshore. Bull Am Assoc Pet Geol 63:286–300

Hunt JH (1979) Petroleum geochemistry and geology. W.H. Freeman, San Francisco, p 617

Hunt JH (1996) Petroleum geochemistry and geology, 2nd edn. Freeman and Company, New York. ISBN 0-7167-2441-3, p 743

Ibrahim MIA (1996) Aptian-Turonian palynology of the Ghazalat-1 Well (GTX-1) Qattara Depression, Egypt. Rev Palaeobot Palynol 94: 137–168

Ibrahim M, Dilcher D, Kholeif S (2009) Palynomorph succession and paleoenvironment in the Upper Cretaceous Abu Gharadig Oil Field, north Western Desert, Egypt. Micropaleontology 55:525–558

Kholeif W, Work JG, and Sanad S, (1986). Melehia: its history and significance: Egyptian General Petroleum Corporation, 8th Exploration and Production Seminar, p. 17–34.

Koeverdon JHV, Karlsen DA, Backer-Owe (2011) Carboniferous nonmarine source rocks from Spitsbergen and Bajornoya: comparison with western Arctic. J Pet Geol 34(1):53–66

Labib M (1984) Contribution to the geology of Upper Cretaceous with special emphasis on Turonian-Senonian sedimentation patterens and hydrocarbon potentials in the Abu Gharadig area, North Western Desert, Egypt. Ph. D. dissertation, Cairo University, Egypt

Mahmoud MS, Moawad AMM (2002) Cretaceous palynology of the Sanhur-1X borehole, north western Egypt. Review Española. Micropaleontology 34(2):129–143

Mahsoub M, ABul-Nasr R, Boukhary M, Faris M (2012) Bio-and sequence stratigraphy of Upper Cretaceous – Palaeogene rocks, East Bahariya Concession, Western Desert. Egypt Geol Croatica 65(2): 109–138

Mansour A, Wagreich M, Gentzis T, Ocubalidet S, Tahoun SS, Elewa AMT (2020a) Depositional and organic carbon-controlled regimes during the Coniacian- Santonian event: first results from the southern Tethys (Egypt). Mar Pet Geol 115:104285

Mansour A, Gentzis T, Carvajal-Ortiz H, Tahoun SS, Wagreich M (2020b) Geochemistry and palynology of the upper Albian at the Abu Gharadig Basin, southern Tethys: constraints on the oceanic anoxic event 1d. Geol J 55:6338–6360

Mansour A, Geršlova E, Sykorova I, Vörös D (2020c) Hydrocarbon potential and depositional paleoenvironment of a Middle Jurassic succession in the Falak-21 well, Shushan Basin, Egypt: Integrated palynological, geochemical and organic petrographic approach. Int J Coal Geol 219:103374

Mansour A, Gentzis T, El Nady MM, Mostafa F, Tahoun SS (2020d) Hydrocarbon potential of the Albian-early Cenomanian formations (Kharita- Bahariya) in the North Western Desert, Egypt: A review. J Pet Sci Eng 193:107440

Mansour A, Gentzis T, Carvajal-Ortiz H, Tahoun SS, Elewa AM, Mohamed O (2020e) Source rock evaluation of the Cenomanian Raha formation, Bakr oil field, Gulf of Suez, Egypt: Observations from palynofacies, RGB-based sporomorph microscopy, and organic geochemistry. Mar Pet Geol 122:104661

Mohamed O, Mahdy F, Tahoun SS (2019) Dinoflagellate cyst biostratigraphy of the Santonian-Oligocene succession of the Drazia-1 well, North Western Desert, Egypt. J Afr Earth Sci 158:103511

Nakhla FM, Dardir AA, Saleh SA and Gad NL, 1992. Distribution and geochemical characters of subsurface coal and kerogen bearing Mesozoic formations and their potentialities to generate oil and gas in North Western Desert (NWD), Egypt. Proceedings of EGPC 11thPetroleum Exploration and Production Conference, EGPC, Cairo, 2:184-198.

Parker JR, 1982.“ Hydrocarbon habitat of Western Desert”, 6th EGPC Conference, Cairo, 1–8p

Peters KE (1986) Guidelines for evaluating petroleum source rock using programmed pyrolysis AAPG Bulletin 70(3). https://doi.org/10.1306/94885688-1704-11D7-8645000102C1865D

Peters K, Cassa M (1994) Applied source rock geochemistry. In: Magoon LB, Dow WG (eds) The petroleum system from source to trap, vol 60. AAPG Memoir, pp 93–117

Ricken W (1996) Bedding rhythms and cyclic sequences as documented in organic carbon-carbonate patterns, Upper Cretaceous, Western Interior, U.S. Sediment Geol 102:131–154

Ruban DA, Zorina SO, Conrad CP (2010) No global-scale transgressive-regressive cycles in the Thanetian (Paleocene): evidence from inter regional correlation. Palaeogeogr Palaeoclimatol Palaeoecol 295: 226–235

Schlumberger (1984).Well evaluation conference of Egypt. Schlumberger Middle East, 201 P.

Schrank E, Ibraheim MI (1995) Cretaceous (Aptian-Maastrchtian) palynology of foraminifera-dated wells (KRM-1, AG-18) in north western Egypt. Berl Geowiss Abh A177:1–44

Sedek MS, Al Mahdy OMM, 2012. Inverted basin analysis and geological modeling, Razzak oil field, Western Desert, Egypt. Arab J Geosci, 1-23. https://doi.org/10.1007/s12517-011-0511-4

Tahoun SS (2012) Palynostratigraphical and paleoenvironmental significance of a palynomorph assemblage from the Cenomanian of north western Desert. Egypt Egypt J Paleontol 12:73–95

Tahoun SS, Mohamed O (2013) Palynology and genetic sequence stratigraphy of the reservoir rocks (Cenomanian, Bahariya formation) in the Salam Oil Field, north Western Desert, Egypt. Cretac Res 45: 342–351

Tahoun SS, Mohamed O (2015) Leiosphaeridia and Pterospermella acritarch genera as shallowing phase indicators in the early Jurassic, North Sinai, Egypt. Arab J Geosci 8:4581–4588

Tahoun SS, Mohamed O (2020) Distribution of peridiniacean dinoflagellate cysts from cores of organic rich shales of the Duwi and Dakhla formations of Egypt. J Afr Earth Sci 170:103892

Tahoun SS, Mostafa TF, Makled WA, Saleh RA (2015) Palynomorph biostratigraphy of the Cretaceous (Hauterivian-lower Cenomanian) of the South Sallum Well, North Western Desert, Egypt. Arab J Geosci 8:9205–9219

Tahoun SS, Deaf AS, Gentzis T, Carvajal-Ortiz H (2018) Modified RGB-based kerogen maturation index (KMI): correlation and calibration with classical thermal maturity indices. Int J Coal Geol 190:70–83

Tissot BP, Welte DH (1984) Petroleum formation and occurrence. A Mew approach to oil and gas exploration. Springer-Verlag, p 538

Tyson BRV (1993) Palynofacies analysis. In: Jenkins DG (ed) Applied Micropaleontology. Kluwer Acad. Pub, Dordrecht, pp 153–191

Tyson RV (1995) Sedimentary organic matter-organic facies and palynofacies. Chapman & Hall, London, 615 pp

Urban LL, Moore LV and Allen ML, 1976. Palynology, thermal alteration and source rock potential of three wells from Alamein area, Western Desert, Egypt. EGPC, 5th Exploration Seminar, 1-34.

Van Krevelen DW (1993) Coal, 3rd edn. Elsevier Science Publishers, Amsterdam

Waples DW (1985) Geochemistry in petroleum exploration (). D. Reidel Publishing Company, Dordrecht, pp 102–108

Yousef M, Moustafa AR, Bosworth W, Helgeson D (2009) Three-dimensional structural model and fault trap analysis of East Bahariya concession, northern Western Desert. Geological Society of Egypt, Cairo, Egypt (Abstract), Egypt

Yousef M, Yousef M, Sehim A (2019) Structural style and evolution of inversion structures of Horus field, Alamein Basin, northern Western Desert of Egypt. Mar Pet Geol 110:55–72

Zobaa MK, Oboh-Ikuenobe FE, Ibrahim MI (2011) The Cenomanian/Turonian oceanic anoxic event in the Razzak Field, north Western Desert, Egypt: Source rock potential and paleoenvironmental association. Mar Pet Geol 28(8):1475–1482